Available online at www.sciencedirect.com

ScienceDirect

Nuclear and Particle Physics Proceedings 273–275 (2016) 1765–1770

www.elsevier.com/locate/nppp

Latest results of NEMO-3 experiment and present status of SuperNEMO

H. Gómez on behalf of NEMO-3 and SuperNEMO collaborations

Laboratoire de l'Accélérateur Linéaire (LAL), Université Paris-Sud 11, 91898 Orsay Cedex (FRANCE).
e-mail: gomez@lal.in2p3.fr

Abstract

The NEMO-3 experiment looked for neutrinoless double beta decay processes from 2003 to 2011 at the Modane Underground Laboratory. Seven isotopes were studied by the simultaneous recording of the energy and track of the event, standing out ^{100}Mo and ^{82}Se since they were the most massive ones. No evidence for neutrinoless double beta decay has been observed, leading to obtain limits on the effective neutrino mass that are among the best to date, specially for the mentioned isotopes.

In addition to the results regarding the effective neutrino mass, NEMO-3 results have shown the physics potential of the tracking + calorimetry technique for the neutrinoless double beta decay search, specially in terms of background rejection capabilities in the energy region of interest. For this reason, the SuperNEMO experiment has been conceived using this technique as one of the so-called new generation experiments. SuperNEMO is at present under construction after a R&D phase (started in 2007) which concluded that all the requirements are achievable. First phase is the construction of a first module that has been started in 2012 and will finish during 2015, when the data taking is expected to start.

A summary of the latest NEMO-3 results, as well as the present status of the SuperNEMO progress (which includes, for example, the development of outstanding detectors for materials radiopurity and radon concentration measurements), will be presented, together with collaboration prospects about the installation, commissioning and operation of the experiment.

Keywords:
Neutrino, double-beta decay, NEMO-3, SuperNEMO

1. Introduction

Double-beta ($\beta\beta$) decay experiments are one of the most active research topics in neutrino physics. The measurement of the neutrinoless mode ($0\nu\beta\beta$) could give unique information on the neutrino nature (Dirac or Majorana) and its absolute mass scale. This decay would also imply the violation of the lepton number conservation and the existence of physics beyond the Standard Model of Particles. The possible Majorana nature of the neutrino (which means that neutrinos are identical to their own antiparticles) supports different theories about the leptogenesis and the observed matter-antimatter asymmetry, and is also related to other theories as the "see-saw" mechanism, which naturally explains the smallness of neutrino masses if compared with other fundamental matter particles.

Several models can describe the $0\nu\beta\beta$ process, proving the Majorana nature of the neutrino. Considering the light Majorana neutrino exchange mechanism, the $0\nu\beta\beta$ process can be written as:

$$[T^{0\nu}_{1/2}(A,Z)]^{-1} = G_{0\nu}(Q_{\beta\beta},Z)|M_{0\nu}(A,Z)|^2|m_{\beta\beta}|^2 \quad (1)$$

where $|m_{\beta\beta}|$ is the effective neutrino mass for the $0\nu\beta\beta$ decay, $|M_{0\nu}(A,Z)|$ is the Nuclear Matrix Element (NME) and $G_{0\nu}(Q_{\beta\beta},Z)$ is the kinematical phase space factor. For the experimental measurement of the $0\nu\beta\beta$ half-life it is important the accurate measurement of the asso-

http://dx.doi.org/10.1016/j.nuclphysbps.2015.09.284

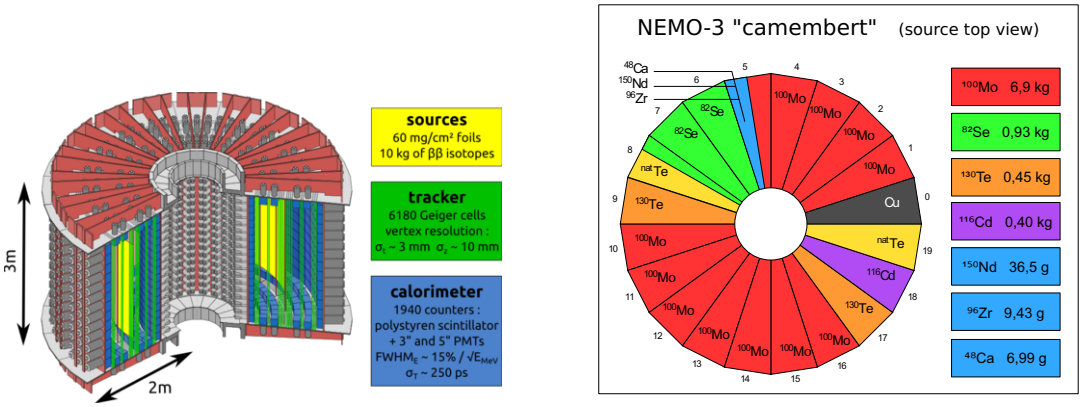

Figure 1: Representation of the NEMO-3 detector section without its shielding and distribution of the double beta sources in the sectors.

ciated two-neutrino double beta decay ($2\nu\beta\beta$) channel. This rare second-order weak process allowed by the Standard Model, represents an irreducible background for the search of the $0\nu\beta\beta$ decay, and its study provides valuable information for the theoretical calculations of the NME as well as for the test of different nuclear models. For these reasons, experiments looking for the $2\nu\beta\beta$ and $0\nu\beta\beta$ decays have been performed during the last years.

2. The NEMO-3 experiment

NEMO-3 was one of the experiments devoted to the study of the $\beta\beta$ decay processes. It operated at the Modane Underground Laboratory (LSM), under a rock overburden of 4800 m.w.e. between 2003 and 2011, when it was decommissioned. The NEMO-3 detector was conceived to be able to fully reconstruct the $\beta\beta$ decay events coming from thin foils (40-60 mg/cm^2) containing different double beta emitters, by the direct detection of the two emitted electrons with a 3D tracking chamber and a segmented calorimeter. Figure 1 shows the design of the NEMO-3 detector and its different components as well as the distribution of the $\beta\beta$ emitters in the different sectors. The foils, that can be metallic or composite (i.e. the isotope is in powder form mixed with PVA glue and sandwiched between two mylar foils), are suspended between two concentric cylindrical tracking volumes composed by 6180 Geiger cells filled with helium (95 %), alcohol (4 %), argon (1 %) and water vapor (0.1 %). This system allows a tracking recostruction precission of σ_t = 2-3 mm transversally to the cells and σ_z = 7-13 mm longitudinally. The tracking volume is surrounded by a calorimeter consisting of 1940 large blocks of plastic scintillator, wrapped with aluminised mylar and Teflon and coupled to low radioactivity 3" and 5" photomultiplier tubes (PMTs). The calorimeter provides a timing resolution of σ = 250 ps while the energy resolution is [14-17] % FWHM for 1 MeV electrons. All the NEMO-3 detector is immersed in a 25 G magnetic field, which curves charged particles tracks making easier their further identification, and shielded from external gamma rays by 19 cm of low activity iron and from neutrons by 30 cm of water with boric acid. A combination of calibrations with radioactive sources, placed inside the detector using 20 calibration tubes located in each sector near the source foils, and a light injection system close to the PMTs, allows the absolute energy scale calibration of all the PMTs as well as the survey of the gain and time variation. A detailed description of the experiment can be found in [1]

NEMO-3 data taking is divided in two phases depending on the radon activity in the tracking chamber: ~30 mBq/m^3 for the high radon phase (Phase 1) and ~5 mBq/m^3 for the low radon one (Phase 2) after the installation of a radon-free air facility at LSM in 2004 flushing a tight tent around the detector.

With these features, NEMO-3 is able to fully reconstruct $\beta\beta$ decay events (Figure 2). These events should be two tracks originated from the same vertex in a source foil, with electron-like curvatures due to the magnetic field, and individually associated to an energy deposit in a calorimeter block. It is possible to measure the energy of each electron as well as their time of arrival and the emission angle at the common vertex. These capabilities can be used for the identification of $2\nu\beta\beta$ and $0\nu\beta\beta$, but also of background events for further rejection.

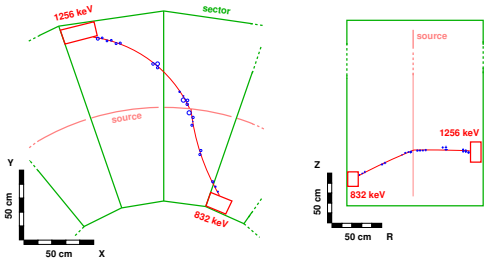

Figure 2: Top and side views of a $\beta\beta$ event with a total energy of 2088 keV reconstructed in NEMO-3. Two electron-like tracks are reconstructed from a single vertex at the source foil, being each track associated to an unique energy deposit in a calorimeter block.

2.1. Background studies

Most important backgrounds for a $\beta\beta$ decay experiment come from the natural radioactivity of the detector materials due to the presence of long half-life isotopes, mainly ^{238}U, ^{235}U, ^{232}Th and ^{40}K and their decay chains. Since NEMO-3 detector is capable to identify different types of particles and event topologies, it is possible to define the origin of a contamination from the tracking and timing information. The fit of the total energy distribution of these types of events, determines the contribution of the natural radioactivity isotopes to the background. Further definition of different analysis channels permits the specific measurement of each type of background.

For the case of the considered external backgrounds, the external γ-ray flux entering the detector can be determined by the detection of the crossing electrons produced by Compton effect in one of the scintillators which escape from the scintillator crossing the whole detector. Due to the presence of the external shielding, the high energy events are mostly produced by the ^{214}Bi, ^{208}Tl and ^{40}K impurities present in the PMTs glass, it exists also a contribution from the ^{60}Co cosmogenic activation of the detector components. At lower energies, there exist also events coming from the β-emitters contaminants of the scintillators or wrapping as ^{40}K, ^{210}Bi from radon deposition or ^{234m}Pa from the ^{238}U chain. In this case, the electron crosses the detector after a backscattering process in the scintillator.

Those events due to source foils contaminants are considered as internal background. For the $0\nu\beta\beta$ search, the main internal backgrounds come from ^{214}Bi (from ^{238}U or ^{226}Ra) and ^{208}Tl (from ^{232}Th or ^{228}Ra) contamination, and also from ^{222}Rn daughters deposition inside the tracking chamber. First two contaminants can be quantified as single β emission or looking at the $\beta - n\gamma$ channel if one or several γ are emitted together with the electron. The radon level can be determined studying the delayed $\beta - \alpha$ events produced by the ^{214}Bi$\rightarrow^{214}$Po cascade of ^{222}Rn chain.

Energy distributions of different analysed events and their corresponding background contributions are presented for illustration in Figure 3. A detailed explanation of the different methods for the background study and its quantification can be found in [2].

2.2. $2\nu\beta\beta$ results

The $2\nu\beta\beta$ decay measurement is interesting not only for the information that it could provide for the theoretical calculations of the NME and for the tests of different nuclear models, but also because it represents an irreducible background for the $0\nu\beta\beta$ search. NEMO-3 has measured the half-life of this process for the seven different isotopes installed, being able to reconstruct the distribution of the total and individual energies and the emission angle between the 2 electrons, as showed in Figure 4 for the case of ^{100}Mo. These plots point out the understanding of the experimental data. Although the result for ^{100}Mo is the most accurate of NEMO-3 since it was the most massive isotope, performing the same analysis for all the isotopes the most precise direct measurements up to now of $2\nu\beta\beta$ decay rates have been obtained. These results are summarised in Table 1.

2.3. $0\nu\beta\beta$ results

The study of the $0\nu\beta\beta$ decay mode for the ^{100}Mo has been performed for the NEMO-3 data with an exposure of 34.7 kg×y. This study has been focused in the [2.8 -3.2] MeV energy window, around the $Q_{\beta\beta}$ value of ^{100}Mo. In this energy window the detection efficiency for the $0\nu\beta\beta$ process is 4.7 % and the background contributions for the different sources are summarised in Table 2. With all these features, no event excess has been observed above the background expectation, so a limit for the half-life of ^{100}Mo $0\nu\beta\beta$ decay can be set. The systematics for this limit mainly come from the uncertainties in the detection efficiency and the background contributions. Dedicated studies evaluates these uncertainties as 7 % for the detection efficiency and 10 % for the background contribution. The limit is obtained using a modified frequentist analysis based on log-likelihood ratio test statistics [8]. For this analysis, the full information of the binned energy sum distribution in the [2.0-3.2] MeV energy window is used for signal and background (Figure 5) together with the statistical and systematic uncertainties and their correlations as described in [8, 6]. The only-background hypothesis is corroborated with a p-value of 64.7 %. The

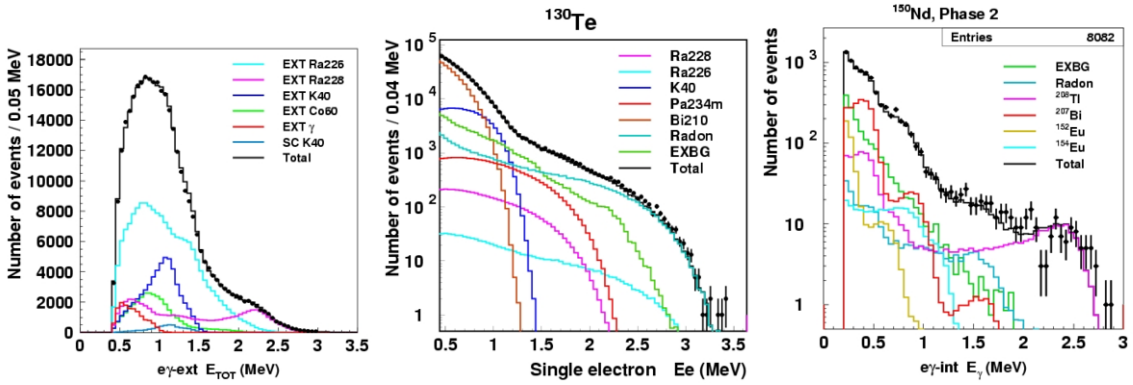

Figure 3: Left: Energy distribution and its background contributions for crossing electrons events (left), single electron events of the ^{130}Te foil (centre) and $\beta - \gamma$ events of the ^{150}Nd foil (right).

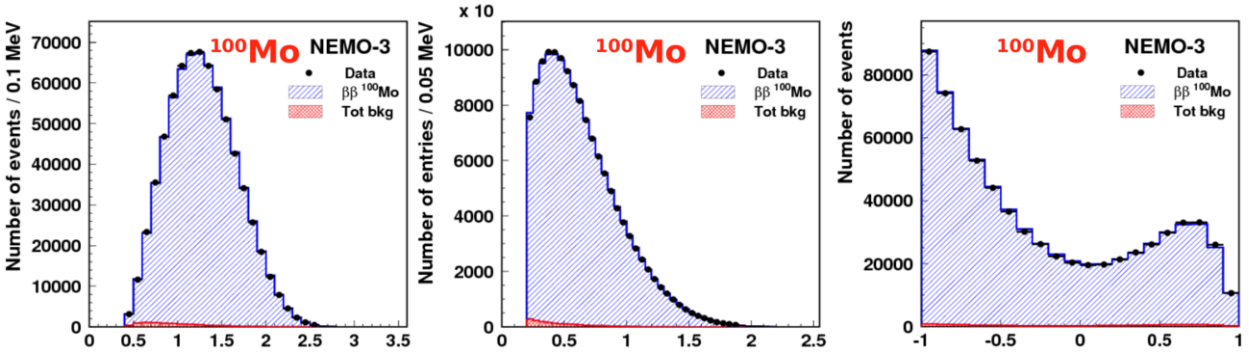

Figure 4: Total energy, individual energy and angular distributions of the ^{100}Mo $2\nu\beta\beta$ events for the Phase 2 of NEMO-3 (3.49 years) [3].

half-life limit for the neutrino mass mechanism of the ^{100}Mo $0\nu\beta\beta$ decay is set to $T^{0\nu}_{1/2} > 1.1\ 10^{24}$ y (90 % C.L.), in agreement with the expected sensitivity of the experiment, which corresponds to a limit on the corresponding effective Majorana neutrino mass of $|m_{\beta\beta}| <$ 300 - 900 meV, depending on the nuclear matrix elements chosen [9, 10, 11, 12, 13] and the phase space calculations [14, 15]. Limits on other lepton number violating mechanisms of ^{100}Mo $0\nu\beta\beta$ decay as right-handed currents in the electroweak Lagrangian or the presence of a Majoron, have been also obtained and can be found in [16]. All the results obtained for the different mechanisms by NEMO-3 are comparable with the best current results obtained with other isotopes.

Another important result coming from the data analysis (and also observed in Figure 5 for the case of ^{100}Mo) is that no events are observed in the [3.2 -10] MeV energy window for NEMO-3 sources containing isotopes with $Q_{\beta\beta}$ lower than 3.2 MeV (i.e. ^{100}Mo, ^{82}Se, ^{130}Te and ^{116}Cd) or without $\beta\beta$ emitters (Cu) during the entire running period, which corresponds to an exposure of 47 kg×y. This result confirms the good features of the tracking+calorimetry approach to perform a background free $0\nu\beta\beta$ experiment, specially for isotopes with a high $Q_{\beta\beta}$ as ^{48}Ca, ^{96}Zr or ^{150}Nd.

3. The SuperNEMO experiment

As evolution of the NEMO-3 experiment, and using the same detection technique combining tracking and calorimetry, SuperNEMO is proposed to achieve a sensitivity for the half-life of $T^{0\nu}_{1/2} > 1\ 10^{26}$ y corresponding to an effective neutrino mass sensitivity of $|m_{\beta\beta}| <$ 40 - 100 meV.

The SuperNEMO experiment is conceived as 20 identical planar modules; each contains 5 kg of $\beta\beta$ isotope distributed in thin foils (40 mg/cm^2) composed by the $\beta\beta$ emitter powder, glue and plastic film or mesh substrate. The baseline of the project chooses ^{82}Se as $\beta\beta$ emitter because its higher $2\nu\beta\beta$ half-life compared to

Table 1: Results of the $2\nu2\beta$ half-life measurements of the seven NEMO-3 isotopes.

Isotope	Mass [g]	$Q_{\beta\beta}$ [keV]	Sig/Bkg	$T_{1/2}$ [years]	Ref.
^{100}Mo	6914	3034	76	7.16 ± 0.01 (stat) $\pm$ 0.54 (syst) 10^{18}	[3]
^{82}Se	932	2995	4	9.6 ± 0.1 (stat) $\pm$ 1.0 (syst) 10^{19}	[4]
^{130}Te	454	2529	0.25	$7.0 \pm 1.4\ 10^{20}$	[5]
^{116}Cd	405	2805	10.3	$2.9 \pm 0.3\ 10^{19}$	
^{150}Nd	37.0	3368	2.8	$9.1 \pm 0.7\ 10^{18}$	[6]
^{96}Zr	9.43	3350	1.0	$2.35 \pm 0.21\ 10^{19}$	[7]
^{48}Ca	6.99	4274	6.8	$4.4 \pm 0.6\ 10^{19}$	

Table 2: Expected background and observed $2e^-$ events in NEMO-3 after a 34.7 kg×y exposure with ^{100}Mo in the total energy range [2.8-3.2] MeV.

Data sets	Phase 1	Phase 2	Combined
External background	< 0.04	< 0.16	< 0.2
^{214}Bi from ^{222}Rn	2.8 ± 0.3	2.5 ± 0.2	5.2 ± 0.5
^{214}Bi internal	0.20 ± 0.02	0.80 ± 0.08	1.0 ± 0.1
^{208}Tl internal	0.65 ± 0.05	2.7 ± 0.2	3.3 ± 0.3
$2\nu2\beta$	1.28 ± 0.02	7.16 ± 0.05	8.45 ± 0.05
Total expected	4.9 ± 0.3	13.1 ± 0.3	18.0 ± 0.6
Data	3	12	15

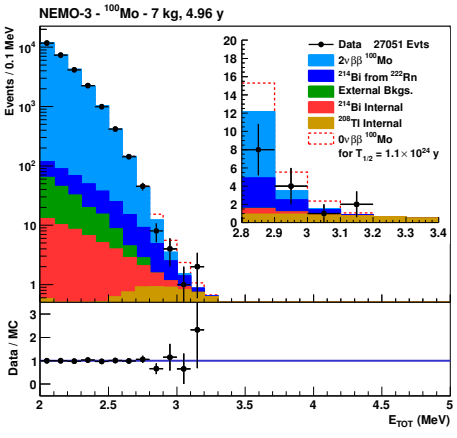

Figure 5: Total energy distribution in the [2.0-3.2] MeV energy window around the $Q_{\beta\beta}$ value of the ^{100}Mo $0\nu\beta\beta$ decay.

the ^{100}Mo one, which induces less background for almost the same $Q_{\beta\beta}$. Other isotopes as ^{48}Ca or ^{150}Nd, have been also considered due to their high $Q_{\beta\beta}$, well above the expected background in the experiment.

Compared with NEMO-3, there are some improvements in order to reach the expected sensitivity. For the calorimeter, the resolution will be 7 % (4 %) FWHM at 1 MeV (3 MeV) improving by a factor 2 the NEMO-3 value. This improvement has been possible by using larger (8") and higher quantum efficiency PMTs directly coupled to the scintillator, better light-yield and transparency scintillators and improved high-voltage divider and digitisation systems. The better performance of the calorimeter will allow to attenuate the background coming from the $2\nu\beta\beta$ decay.

The tracker amelioration mainly relies on the reduction of the radon inside the tracker volume. To achieve this reduction it is necessary an exhaustive control of the radon-tightness and radon-emanation of the different materials conforming the tracker. With this purpose, the collaboration has developed different detectors to measure and control these parameters. After the installation of the tracker modules, the remaining radon concentration activity can be assured to be at the level of 0.15 mBq/m^3, measured by a dedicated radon concentration line. In addition, first prototypes show that the tracking resolution has been also improved from σ_t = 2-3 mm and σ_z = 7-13 mm in NEMO-3 to 0.7 and 10 mm respectively.

The third main background that must be reduced to improve the sensitivity is that coming from the internal contamination of the source foils, mainly ^{208}Tl and ^{214}Bi. To do that, all the materials and processes, as the purification of the selenium powder, have to be strictly controlled in terms of radiopurity. SuperNEMO estimations limit the contamination of the source foils to 2 (10) μBq/kg in ^{208}Tl (^{214}Bi), which are levels that can not be achieved using conventional radiopurity measurements techniques as γ spectroscopy using high-purity germa-

nium detectors. For this reason the collaboration developed a dedicated detector to measure ultra-low radioactivity levels in the SuperNEMO source foils, reaching the required sensitivity. This detector is called BiPo and its detection principle is based on the detection of the delayed $\beta - \alpha$ coincidences that happen in the ^{212}Bi$\rightarrow^{212}$Po and ^{214}Bi$\rightarrow^{214}$Po cascades. A description of this detector, fully operative at the Canfranc Underground Laboratory (LSC) since January 2013, can be found in [17].

4. Present status: The SuperNEMO demonstrator

The SuperNEMO collaboration is currently involved in the construction of the first module of the detector called demonstrator (Figure 6). This detector will hold 7 kg of ^{82}Se distributed in 53 mg/cm^2 foils and following the SuperNEMO specifications it will be able to reach the NEMO-3 sensitivity after only 5 months of data taking. If as expected, no background is registered in the $0\nu\beta\beta$ after 2.5 years (17.5 kg×y exposure), the half-life will increase up to $T^{0\nu}_{1/2} > 6.5\ 10^{24}$ y, leading to a mass sensitivity of $|m_{\beta\beta}| < 200$ - 400 meV (90 % C.L.).

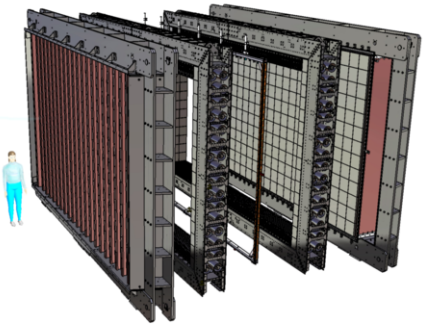

Figure 6: Representation of the SuperNEMO demonstrator opened.

At present, the demonstrator calorimeter is under construction with the preparation of the optical modules composed by the PMTs and the scintillator blocks. The mechanical structure and the PMT magnetic shields are at the end of the production stage like the front-end digitizing electronics. For the tracker, first of the quarters has been assembled and its radon emanation tested, this quarter has been populated with the drift cells produced by a wiring robot. 5.5 kg of ^{82}Se have been purchased and purified. The source materials are under selection process with the BiPo detector and the first two sources are currently under measurement. The calibrations systems (source deployment and light injection) have demonstrated the stability requirements. The integration of the demonstrator at LSM, in the place of NEMO-3, will start at the autumn 2014 and the physics data taking should start in the second half of 2015.

5. Summary

The NEMO-3 experiment had unique capabilities for track reconstruction which permitted the full signature of $\beta\beta$ events and efficient background rejection. After 34.7 kg×y exposure, no evidence for the $0\nu\beta\beta$ of ^{100}Mo is found. Taking into account statistical and systematic uncertainties, this can be translated to a limit on the half-life for the light Majorana neutrino mass mechanism of $T^{0\nu}_{1/2} > 1.1\ 10^{24}$ y (90 % C.L.) and to a limit on the corresponding effective Majorana neutrino mass of $|m_{\beta\beta}| <$ 300 - 900 meV, depending on the NME chosen. In addition to these results, NEMO-3 revealed the tracking + calorimetry detection technique as background free at high energy, which encourage its application for future experiments planning to use high $Q_{\beta\beta}$-value isotopes like ^{48}Ca, ^{96}Zr or ^{150}Nd.

As evolution of the NEMO-3, the SuperNEMO experiment is being performed. As first phase, a first module called demonstrator is under construction, which will hold 7 kg of ^{82}Se. It will be able to reach NEMO-3 sensitivity for the $0\nu\beta\beta$ decay in only 5 months. If no background event in the $0\nu\beta\beta$ region is detected after 2.5 years of data taking, which implies an exposure of 17.5 kg×y, the half-life sensitivity will be increased up to $T^{0\nu}_{1/2} > 6.5\ 10^{24}$ y (90 % C.L.) leading to a mass sensitivity of $|m_{\beta\beta}| < 200$ - 400 meV. The physics data taking of the demonstrator will be expected to start during the second half of 2015.

References

[1] R. Arnold et al, Nucl. Instr. and Meth. A 536 (2005) 79
[2] J. Argyriades et al, Nucl. Instr. and Meth. A 606 (2009) 449
[3] L. Simard, J. Phys.: Conf. Series 375 (2012) 042011
[4] R. Arnold et al, Phys. Rev. Lett. 95 (2005) 182302
[5] R. Arnold et al, Phys. Rev. Lett. 107 (2011) 062504
[6] J. Argyriades et al, Phys. Rev. C 80 (2009) 032501
[7] J. Argyriades et al, Nucl. Phys. A 847 (2010) 168
[8] T. Junk, Nucl. Instr. and Meth. A 434 (1999) 435
[9] J. Suhonen and O. Civitarese, J. Phys. G 39 (2012) 124005
[10] F. Šimkovic et al, Phys. Rev. C 87 (2013) 045501
[11] J. Barea and F. Iachello, Phys. Rev. C 79 (2009) 044301
[12] P. K. Rath et al, Phys. Rev. C 82 (2010) 064310
[13] T.R. Rodriguez and G. Martinez-Pinedo, Phys. Rev. Lett. 105 (2010) 252503
[14] J. Kotila and F. Iachello, Phys. Rev. C 85 (2012) 034316
[15] S. Stoica and M. Mirea, Phys. Rev. C 88 (2013) 037303
[16] R. Arnold et al, Phys. Rev. D 89 (2014) 111101
[17] H. Gómez, Nucl. Instr. and Meth. A 718 (2009) 52